Kinetic Studies of Geminate Polaron Pair Recombination, Dissociation, and Efficient Triplet Exciton Formation in PC:PCBM Organic Photovoltaic Blends

ARTICLE *in* THE JOURNAL OF PHYSICAL CHEMISTRY C · FEBRUARY 2013

Impact Factor: 4.77 · DOI: 10.1021/jp208820g

3 AUTHORS:

Edward William Snedden
Science and Technology Facilities Council
16 PUBLICATIONS **82** CITATIONS
SEE PROFILE

Andy Monkman
Durham University
416 PUBLICATIONS **9,852** CITATIONS
SEE PROFILE

Fernando Dias
Durham University
66 PUBLICATIONS **1,440** CITATIONS
SEE PROFILE

THE JOURNAL OF PHYSICAL CHEMISTRY C

Article

pubs.acs.org/JPCC

Kinetic Studies of Geminate Polaron Pair Recombination, Dissociation, and Efficient Triplet Exciton Formation in PC:PCBM Organic Photovoltaic Blends

Edward W. Snedden,* Andrew P. Monkman, and Fernando B. Dias

Organic Electroactive Materials Group, Department of Physics, Durham University, South Road, Durham DH1 3LE, United Kingdom

Supporting Information

ABSTRACT: The recombination and dissociation of geminate polaron pairs (GPPs) in bulk-heterojunction blends of the dye molecule 1,4,8,11,15,18,22,25-octabutoxy-29*H*,31*H*-phthalocyanine (PC) with the electron acceptor [6,6]-phenyl-C61-butyric acid methyl ester (PCBM) is studied using femtosecond transient absorption spectroscopy. The kinetics of the GPP state is dominated by efficient recombination to the triplet state of the PC, which competes with GPP dissociation and acts to fundamentally reduce the total number of free polarons generated in the blend. Both recombination and dissociation are strongly dependent on the blend morphology, with increased free polaron yields obtained by creating percolation pathways for polarons to move away from interfacial regions. Under such conditions, however, rapid exciton decay within PC domains occurs before the onset of electron transfer and acts to further reduce the free polaron yield. The consequences of these factors on the operation of solar cells using ternary blends for near-infrared sensitization are discussed.

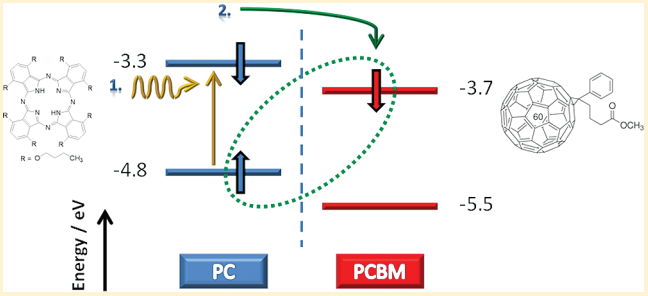

1. INTRODUCTION

One of the key challenges in the advancement of organic photovoltaic (OPV) technology is the development of donor and acceptor materials that efficiently capture radiation across the full solar spectrum. Significant research has been placed into OPV systems based on bulk-heterojunction blends of the conjugated polymer region-regular poly(3-hexylthiophene) (P3HT) with the electron acceptor [6,6]-phenyl-C61-butyric acid methyl ester (PCBM). To date, this remains one of the most efficient single junction polymer:PCBM OPV systems on record, with reported power conversion efficiencies approaching 5%.[1,2] It is, however, noteworthy that the P3HT:PCBM system has negligible absorption in the NIR spectral region, where the Sun's photon flux is at a maximum. OPV blends of low band gap polymers with C_{70} derivative [6,6]-phenyl-C71-butyric acid, in which the absorption is more intense than C_{60} PCBM, have been used to enhance solar photon capture in OPV devices, with reported power conversion efficiencies in excess of 7%.[1,3] Another successful approach to extending solar capture has been the use of phthalocyanine (PC) small molecules, which display intense absorption in the NIR region.[4] These dye molecules can either be employed as donor materials in OPV blends using PCBM as the acceptor[5,6] or in ternary blends with conjugated polymers such as P3HT, where they act as sensitizers to extend solar capture.[7−12] PC molecules can also act to improve the efficiency of ternary blends via the so-called antenna effect, whereupon exciton, harvesting in the polymer is increased as a consequence of long-range Förster energy transfer from the host to PC.[10,12−14]

Despite their emergence within the field, there are only a limited number of detailed photophysical studies of charge generation in binary and ternary PC solar cell blends,[11,12] particularly those focusing on charge generation at the PC:PCBM interface. The processes of exciton dissociation and charge separation play a vital role in determining the performance of OPV devices.[15−17] Of particular interest is the fate of the transient geminate polaron pair (GPP) intermediate formed at the donor/acceptor interface following electron transfer. This bounded intermediate state is thought to be the precursor for the creation of free carriers and thus has to undergo a further process of dissociation to generate free charges, which can then move to the electrodes to be collected as photocurrent.[17−19] Different nomenclature has been used within in the literature to describe this state, such as charge-transfer state, geminate polaron pair, and bound polaron pair.[20−24]

The interplay between GPP recombination and dissociation defines the separation yield of an OPV blend, which in turn goes toward determining the extracted photocurrent.[16] It is clear at a basic level that in order to improve the separation yield, dissociation must be favored over recombination. A

Received: September 13, 2011
Revised: January 16, 2012
Published: January 17, 2012

detailed understanding of these individual processes is therefore of significant interest. GPP recombination can either occur to the singlet or triplet[18,25] manifold of the donor as a result of electron back-transfer or through direct recombination across the donor/acceptor interface. This latter process can either occur radiatively, resulting in a weak photoluminescence band on the red edge of the polymer fluorescence, or non-radiatively.[20−24] The process of GPP dissociation is less well understood and is thought to be determined by a large number of different factors, including nanomorphology, entropy, quantum interactions at the donor−acceptor interface, and the influence of internal electric fields, to name but a few; the reader is referred to several of the excellent review papers on the subject.[15−17]

In this work, we report on kinetic studies of the GPP state in PC:PCBM OPV blends, identifying the relevant recombination and decay pathways. The influence of morphology on these processes is considered, with particular attention given to the various factors that influence the free polaron yield. The consequences of these factors on the operation of PC:PCBM and dye-sensitized solar cells is also discussed.

2. EXPERIMENTAL SECTION

Base solutions of 1,4,8,11,15,18,22,25-octabutoxy-29*H*,31*H*-phthalocyanine (PC, Sigma Aldrich, 95%) and [6,6]-phenyl-C61-butyric acid methyl ester (PCBM, Sigma Aldrich, >99%) were prepared by dissolving the materials in chlorobenzene under heating and stirring. These solutions were combined together to produce mixtures of PC and PCBM (1:0.1 and 1:1 w/w, 10 mg·ml^{-1} dye content). Solid thin films were prepared by spinning on to quartz substrates (1500 rpm, 60 s). Thermal annealing of all blend films was performed by heating in a vacuum oven at 150 °C for 15 min. The absorption spectra of these films are presented in Figure 1.

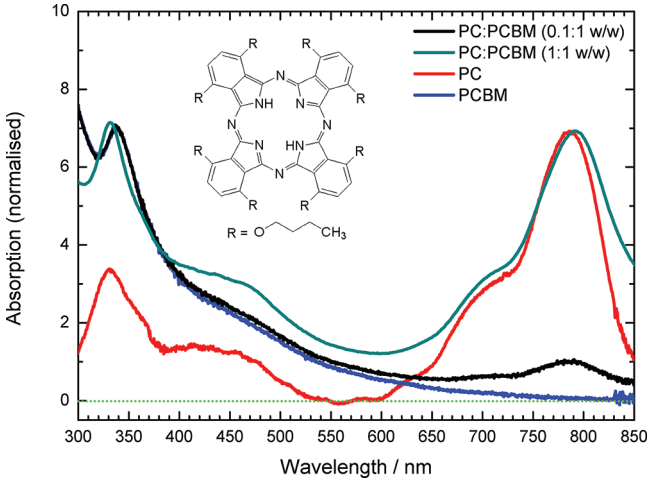

Figure 1. Normalized absorption spectra of solid thin films; pristine PC (red), pristine PCBM (blue), 0.1:1 (w/w, black), and 1:1 (green) PC:PCBM (both bulk-heterojunction blends). The chemical structure of PC is included as an inset.

Ultrafast transient absorption spectroscopy was performed using a conventional femtosecond noncolinear pump−probe setup. Ultrafast laser pulses (180 fs, 4 μJ, 100 kHz repetition rate) at 780 nm were generated using a Coherent Mira900-f Ti:Sapphire femtosecond oscillator in conjunction with a Coherent RegA 9000 laser amplifier. The amplifier output was used to drive a Coherent 9400-OPA, with the single wavelength (780 nm) and white-light supercontinuum (470−1000 nm) outputs used to generate pump and probe, respectively. The variable delay between pump and probe pulses was controlled by means of a motorized linear translation stage (Newport). A variable $\lambda/4$ waveplate was introduced to the pump path and used to control the relative orientation of the pump polarization with respect to the probe. The pump was oriented at 54.7° (magic angle) with respect to the probe to ensure the transient data obtained was independent of polarization.

Thin film samples were mounted in a closed-cycle Cryomech helium pulse tube cryostat under a dynamic vacuum of <10^{-5} mbar. Spectral components in the white-light probe were resolved using a monochromator (Bentham M300) prior to detection using an amplified silicon photodiode. The relative transmission change $\Delta T/T$ of the probe beam was measured using a lock-in amplifier referenced to the mechanically chopped pump beam.

Details of steady-state absorption spectroscopy and electrochemistry are given in the Supporting Information.

3. RESULTS AND DISCUSSION

3.1. Excited-State Kinetics in PC:PCBM (0.1:1 w/w) Blend Films. The transient absorption spectrum of the PC:PCBM (0.1:1 w/w) blend film is presented in Figure 2,

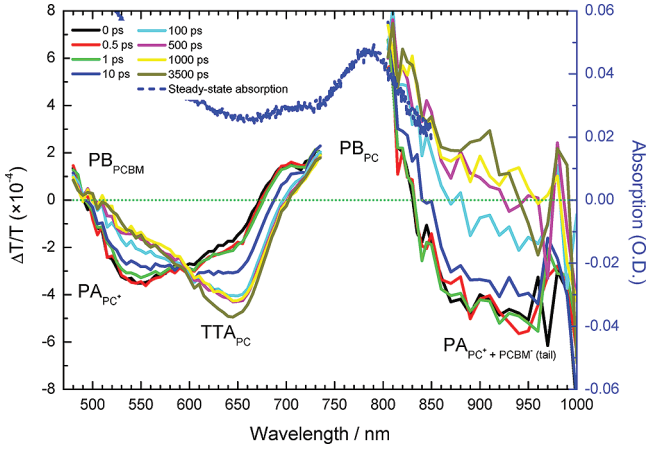

Figure 2. Transient absorption spectrum of PC:PCBM (0.1:1 w/w) blend, measured at different pump−probe delay times as marked (780 nm excitation, 30 μJ·cm^{-2}). Bands corresponding to photoinduced absorption (PA), photobleaching (PB), and triplet−triplet absorption (TTA) are marked. The ground-state absorption of the blend (blue dashed line, O.D., optical density) has been included for reference. Note that data has been rejected in the region of 780 nm due to saturating content in the probe beam.

as measured at a range of different pump−probe delay times. Following excitation of the PC content (780 nm, 30 μJ·cm^{-2}), four distinct bands can be identified at 0 ps; photobleaching ($\Delta T/T > 0$) at 470 nm, photoinduced absorption ($\Delta T/T < 0$) at 540 nm, photobleaching at 780 nm, and photoinduced absorption at 950 nm. The photobleaching at 470 and 780 nm can be uniquely identified as such as both regions clearly overlap with the ground-state absorption spectrum of the PCBM and dye components of the blend, respectively, as demonstrated in Figure 2. The photoinduced absorption band at 920 nm is unique to the blend film and cannot be identified

dx.doi.org/10.1021/jp208820g | J. Phys. Chem. C 2012, 116, 4390−4398

in the transient absorption spectra of the pristine components (see Figure I, Supporting Information) and therefore can only arise as a result of electron transfer between the PC and PCBM moieties. The decay of the photoinduced absorption at 920 nm is noted to be similar to that at 540 nm. The decay of these bands is matched by the build-in of a new photoinduced absorption band at 640 nm. An isosbestic point at 600 nm is indicative of a one-to-one relationship between the decay of the photoinduced absorption at 540 nm and the build-in at 640 nm. Note that there is also prominent overlap between the photoinduced absorption bands at 540 and 640 nm and the photoinduced absorption band at 920 nm with the PC photobleaching; this can be readily observed by comparing the transient absorption spectra at 0 and 3500 ps.

As the PA band at 950 nm is formed within the minimum time resolution of our system (400 fs) and cannot be attributed to any PC or PCBM excitonic species, it is attributed to the PA of polarons formed following electron transfer. This is consistent with the observation of PCBM PB on the same time scale; note that for excitation at 780 nm, direct photoexcitation of the PCBM content is not possible, and therefore, the observation of PC PCBM is only consistent with the ultrafast formation of $PCBM^-$ anions. Furthermore, no stimulated emission (SE) from the singlet exciton population, which is observed in the pristine film at 880 nm, can be detected at 0 ps. In summary, there is a great deal of evidence indicating the efficient quenching of the PC singlet population due to electron transfer within 400 fs. This is consistent with the reported lifetime of electron transfer of 40 fs in a conjugated polymer/PCBM blend.[26] Note that exciton migration is not required as a precursor to electron transfer and polaron formation; for the low ratio of PC to PCBM, all excitons are generated within the quenching radius of a suitable PCBM domain.

Following on from the discussion above and taking the fact that the $PCBM^-$ anion PA is documented within the literature to occur at ~1020 nm,[27] we attribute the PA band at 950 nm to the PC^+ cation. This assignment is confirmed in the analysis of the corresponding single-wavelength decay kinetics, which are discussed below. Note that some small overlap with the tail of the $PCBM^-$ anion is, however, expected at 1000 nm. Further details of this assignment are given in Figure I-B of the Supporting Information.

The discussion of Figure 2 is supplemented by an analysis of the TA kinetics at single wavelengths corresponding to the key PA and PB bands discussed above. The kinetics obtained at 540, 640, and 930 nm are presented in Figure 3A. A simple correction procedure has been applied to the kinetic data obtained at 540 and 640 nm to account for the spectral overlap between the two PA bands in that vicinity, as discussed above; the details of this process are included in the Supporting Information. The negative background in the 930 nm data is a consequence of the aforementioned overlap at that wavelength with the PC PB. From Figure 3A, it is first clear that the decay of the PA bands at 540 and 930 nm are identical. This can be seen directly from Figure 3A and is confirmed using the results of independent multiexponential fitting at each wavelength, the details of which are included in the Supporting Information. We therefore also attribute the PA at 540 nm to a transition of the PC^+ cation.

The PA at 640 nm (as observed at 3.5 ns) is identical to the triplet−triplet (T_1−T_N) absorption (TTA) band of PC, as discussed in previous studies[28] and is hence identified as thus.

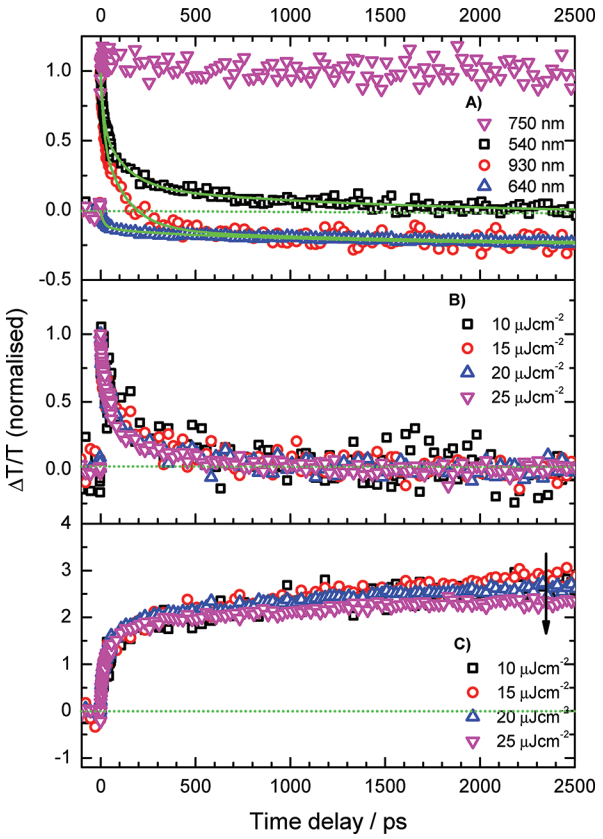

Figure 3. Normalized single wavelength TA kinetics from the PC:PCBM (0.1:1 w/w) blend (780 nm excitation). (A) Polaron and triplet kinetics at 540, 640, and 930 nm (as marked), including global multiexponential fit (green lines); (B) polaron kinetics at 540 nm, obtained at a range of different excitation fluences; and (C) triplet kinetics at 640 nm, obtained for the same fluences.

The long lifetime of the band (no decay is observed up to 3500 ps) is also consistent with this assignment. Following these assignments, the isosbestic point at 600 nm is indicative of a one-to-one relationship between the decay of PC^+ polarons and the build-in of PC triplet excitons. As part of this process, there is a conservation of states in the PC moieties and as such no PB decay, which is a specific measure of the ground-state recombination process, is expected. As can be seen in Figure 1, this is indeed the case. Note that the decay of the PC PB at 700 nm can be attributed to overlap with the PC TTA band.

It is clear from Figure 3 that the decay at long delay times (<1 ns) of the PA bands at 540 and 950 nm is very similar to the build-in of the PC TTA at 640 nm; the data at 640 nm has been renormalized to emphasize this point. This is consistent with the presence of the isosbestic point at 600 nm, as discussed above. Taking all points into consideration, a global exponential analysis of the data at 540, 640, and 930 nm is warranted. The results of this process are included in Figure 3A and demonstrate an excellent fit to the data, with three lifetime components of (16 ± 2), (120 ± 10), and (1100 ± 300) ps obtained (Table 1).

The intensity dependence of the single-wavelength kinetics at 540 and 640 nm are presented in Figure 3B and C, respectively. It is clear from a direct inspection of Figure 3B that the decay at 540 nm is intensity independent, signifying geminate recombination. We therefore move to formally classify the PA at 540 nm (and by extension, that at 950 nm) to

dx.doi.org/10.1021/jp208820g | J. Phys. Chem. C 2012, 116, 4390−4398

Table 1. Results of Global Fitting to Selected Data from Figure 3A (0.1:1 w/w Blend)[a]

wavelength nm)	a_1 (%)	τ_1 (ps)	a_2 (%)	τ_1 (ps)	a_3 (%)	τ_3 (ps)
540	43 ± 9	16 ± 2	18 ± 8	120 ± 10	40 ± 6	1200 ± 300
640	35 ± 3	16 ± 2	54 ± 3	120 ± 10	11 ± 2	1200 ± 300
930	37 ± 3	16 ± 2	42 ± 3	120 ± 10	22 ± 2	1200 ± 300

[a]Data obtained using the following model:

$$\frac{\Delta T}{T}(t) = A_1\, e^{-t/\tau_1} + A_2\, e^{-t/\tau_2} + A_3\, e^{-t/\tau_3}$$

All component amplitudes are presented as a percentage of the total amplitude, as calculated according to $a_i = A_i/(\Sigma_{j=1}^{3} A_j)$.

characterize the decay of the geminate polaron pair (GPP) species, formed following electron transfer from PC to PCBM. Following the established convention,[17] we are unable to strictly classify the states as charge-transfer species as we do not detect any evidence of so-called charge-transfer emission due to experimental limitations. This does not, however, detract from the significance of our observations.

Following inspection of Figure 3C, it is clear that the PC TTA kinetics at 640 nm are intensity dependent, with a decay component of the order of 1 ns appearing at higher fluences. This is consistent with the assignment of the PA at 640 nm to triplet excitons and is reflective of triplet−triplet annihilation.[29−31] Involving what is essentially a contact process between two excitons, the effectiveness of triplet−triplet annihilation is dependent on the excitation density (and thus by extension, the excitation fluence), becoming more prominent at higher fluences.

In summary, the data of Figure 3 cooperatively reinforces the analysis of Figure 2, namely, the assignment of PC^+ polarons and triplet excitons to the PA bands at 540/950 and 640 nm, respectively, and establishes that the one-to-one correlation discussed above is reflective of interfacial GPP recombination directly to the triplet energy level of the PC. The efficiency of PC triplet exciton formation can be measured by considering the kinetics of the PB recovery, as measured at 750 nm (Figure 3A), and the polaron decay at 540 nm. The data at 750 nm confirms the observations of the TA spectra in Figure 2, namely, there is almost no PB decay on a nanosecond time scale. A very weak decay component of the order of 100 ps can just be observed, but is too small in amplitude to be analyzed accurately using an exponential fit. As such, it is possible to infer that there is no significant ground-state recovery process active in the system on a nanosecond time scale.

Interestingly, there is also no evidence of the generation of any free polarons; that is, those states which have overcome any interfacial binding energy and are characterized by decay kinetics on a microsecond time scale.[32,33] A measure of the free polaron yield (with respect to the initial GPP population) can be taken by comparing the magnitude of the polaron PA at 0 ps to that at much longer times (3.5 ns). To provide an accurate measure of this, however, it is first necessary to ensure that the polaron PA does not overlap with the transition of any other state. We make this measurement at 950 nm; at this wavelength there is no overlap of the polaron PA with the PC PB, as confirmed in the pristine PC material (see Figure I, Supporting Information). It is clear from Figure 2 that the polaron PA at 950 nm decays to a background of zero, which is indicative of no free polaron formation.

Developing this point further, the very long-lived ground-state recovery term present in the PC PB recovery at 750 nm can only be attributed to PC triplet excitons. To clarify, the decay of the PC triplet has been measured to occur on a microsecond time scale, which is too long to be observed within the limits of our apparatus.[28,34] It is possible to determine the yield of triplet excitons (Φ_T, with respect to the initial photoexcitation population) by taking the ratio of the PB magnitude at 0 ps, to that at 3500 ps. This calculation is based on the principle that the photobleaching measures the absence of all states from the ground-state and can thus be taken as an effective measure of the number of holes formed.[35] A hole can be associated equally with a singlet exciton, triplet exciton, or polaron, and as such, the photobleaching kinetics measure the ground-state recovery of all these states equally at the same time. As we have established that the only states existing at 3500 ps are triplet excitons, the yield of triplet excitons follows as the ratio of the amplitudes expressed above, yielding Φ_T = [100 ± 10] %. Further details are given in the Supporting Information.

Scheme 1 summarizes the model of GPP recombination and triplet exciton formation in the PC:PCBM (0.1:1 w/w) blend.

Scheme 1. Summary of Excited-State Kinetic Processes in the PC:PCBM (0.1:1 w/w) Film[a]

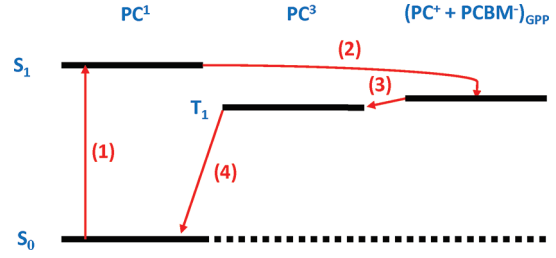

[a]Following photoexcitation of the PC (1), electron transfer (2) from PC to PCBM occurs within 100 fs, resulting in the formation of PC^+/$PCBM^-$ geminate polaron pairs. The GPPs recombine (3) with a high efficiency to the triplet of the PC. The recombination process occurs with a range of lifetimes (of the order of 10 to 1000 ps), which is reflective of a distribution of electron-hole separations within the GPP manifold. Triplet recombination to the ground-state (4) then follows on a microsecond time scale.

Given the efficient recombination of the GPP state to the triplet of the PC, standard experimental determination of the GPP energy (E_{GPP}) using the energy of radiative recombination was not possible. Instead, a basic consistency check was performed by calculating an upper bound for the binding energy of the GPP state. The total energy of the GPP state is given in eq 1 and is related to the energy difference between the lowest unoccupied molecular orbital (LUMO) of the donor and highest occupied molecular orbital (HOMO) of the

dx.doi.org/10.1021/jp208820g | J. Phys. Chem. C 2012, 116, 4390−4398

acceptor, offset by the coulomb binding energy (E_B) of the pair.[17]

$$E_{GPP} = (E^{PCBM}_{LUMO} - E^{PC}_{HOMO}) - E_B \quad (1)$$

In-house cyclic voltammetry measurements were used to determine the HOMO of the PC (−4.82 eV) and LUMO of the PCBM (−3.70 eV), giving E_{GPP} = 1.12 eV − E_B. Taking the literature value from the triplet energy level of PC (0.98 eV)[36] and the fact that recombination to the triplet can only occur with a measurable probability if the initial and final states are approximately within k_BT (~20 meV) of each other, the binding energy yields an upper bound of $E_B \leq [0.14 \pm 0.02]$ eV. This value is of the same order of magnitude as those reported for the binding energy of the GPP state in other donor/acceptor systems,[17,18] confirming the feasibility for GPP recombination to the PC triplet in the PC:PCBM system.

A description of Scheme 1 is now the following:

(1) Photoexcitation of the PC results in the formation of singlet excitons.
(2) The singlet exciton population is rapidly and efficiently quenched (<400 fs) as a consequence of electron transfer from PC to PCBM, resulting in the formation of PC^+/$PCBM^-$ GPPs. There is no evidence for exciton migration as a precursor to polaron formation; at this low doping ratio, 100% of singlet excitons are photogenerated within the capture radius of a PCBM domain.
(3) The GPPs recombine with a high (~100%) efficiency to the triplet of the PC. This process occurs with a range of lifetimes, spanning orders of 10 to 1000 ps. No free polaron generation is observed.
(4) The PC triplet excitons recombine to the ground-state with a lifetime of the order of microseconds.

The key issue that arises from Scheme 1 is the nature of GPP recombination, which occurs with a range of lifetimes, as opposed to a single lifetime. We attribute this to a distribution of electron−hole distances in the GPP manifold. For example, whereas some states are tightly bound and can give rise to 10 ps recombination lifetimes, the recombination of larger GPPs must be proceeded by a rate-limiting diffusive stage in which electron and hole move back toward the interface. Very similar concepts have been proposed in recent studies by Gélinas et al.[37] and Johansson et al.[11,38]

A distribution of GPP states and subsequently a distribution of recombination lifetimes is a natural concept and reflective of the complexity of interfacial interactions in a bulk-heterojunction donor/acceptor system. Indeed, it is likely that the process of GPP recombination is influenced simultaneously both by spatial and mobility factors. The fact that we only resolve three lifetime components in our analysis is reflective of the signal-to-noise limitations of the fitting process. We stress, however, that, at this point in our study, using the fitting process to gain an understanding that there is a one-to-one relationship between GPP recombination and triplet exciton formation and that recombination occurs with a range of lifetimes, is sufficient for discussion.

At a more general level, the observation of efficient GPP recombination to the PC triplet manifold is significant. It is clear that in order to promote efficient OPV performance, efficient GPP recombination must be limited at the expense of dissociation, in order to favor high operating photocurrent and open-circuit voltage conditions.[16,17,39] One fact that may strongly influence the GPP recombination kinetics is the blend morphology; following electron-transfer in the 0.1:1 bulk heterojunction blend, the probability for the PC^+ cation to escape from the interface is expected to be limited by an absence of a suitable percolation path. To investigate this point further, kinetic studies were performed on a PC:PCBM (1:1 w/w) blend; these results are now discussed below.

3.2. Excited-State Kinetics in PC:PCBM (1:1 w/w) Blend Films. The TA spectrum of the PC:PCBM (1:1 w/w) blend film is presented in Figure 4A, as measured at a range of different pump−probe delay times following excitation at 780 nm (10 $\mu J \cdot cm^{-2}$). Note that the incident fluence has been adjusted as compared to the corresponding measurement for the 0.1:1 blend film in order to maintain the same excitation density. Immediately following excitation at 0 ps, the spectrum is identical, in both form and magnitude, to that of the 0.1:1 blend at the corresponding time (see Figure IV-A, Supporting Information). Following the analysis of section 3.1, we hence immediately proceed to identify PA bands corresponding to

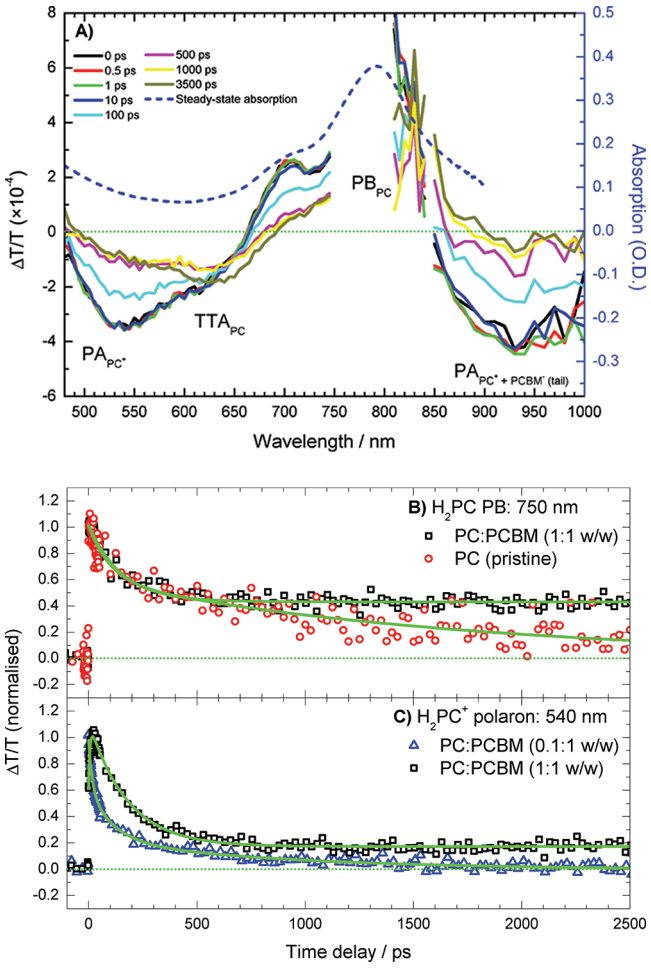

Figure 4. (A) Transient absorption spectrum of PC:PCBM (1:1 w/w) blend, measured at different pump−probe delay times as marked (780 nm excitation, 10 $\mu J \cdot cm^{-2}$). Note that the incident fluence has been adjusted with respect to the 0.1:1 blend film (Figure 2) in order to maintain the same excitation density. The ground-state absorption of the blend (blue dashed line) has been included for reference. (B) Comparison of the PB recovery (750 nm) in the PC:PCBM (1:1 w/w) film (black squares) with that in pristine PC (red circles). (C) Comparison of the PC^+ polaron PA kinetics (~540 nm) in the 0.1:1 (blue triangles) and 1:1 (black squares, extracted) blends.

dx.doi.org/10.1021/jp208820g | J. Phys. Chem. C 2012, 116, 4390−4398

Table 2. Results of Multiexponential Fitting to the PC^+ Polaron Kinetics in the 0.1:1 and 1:1 (w/w) Blend Films, As Measured at 540 nm[a]

blend (w/w)	wavelength (nm)	A_1	τ_1 (ps)	A_2	τ_2 (ps)	A_3	τ_3 (ps)
0.1:1	540	0.37 ± 0.02	16 ± 2	0.42 ± 0.03	120 ± 10	0.22 ± 0.02	1200 ± 300
1:1	540	−0.52 ± 0.02 (rise)	6.3 ± 0.5	0.95 ± 0.01	177 ± 5	0.171 ± 0.003	long

[a]Data was analyzed using the following model:

$$\frac{\Delta T}{T}(t) = A_1\, e^{-t/\tau_1} + A_2\, e^{-t/\tau_2} + A_3\, e^{-t/\tau_3}$$

The results of fitting to the singlet exciton PA kinetics in the pristine PC film (1:0), as measured at 640 nm, are included for reference (see Figure II, Supporting Information, for original data).

PC^+ polarons at 540 and 950 nm, in addition to PB of the PC ground state at 780 nm. Both polaron bands are observed to decay on a 100 ps time scale. In contrast, however, to that recorded in the 0.1:1 film, the PB band of the 1:1 film is also observed to decay on the same time scale, indicating that there is a new process active in the blend that results in the recovery of the PC ground state. Furthermore, the polaron PA at 950 nm decays to a nonzero background, which is indicative of free polaron formation. Following the discussion of section 3.1 above and again taking the PA at 950 nm to be pure representative of the polaron kinetics, it can be determined that the free polaron yield (Φ_{FP}) in the 1:1 film is (12 ± 4) %.

After 500 ps, a new PA band at 640 is resolved and continues to build-in up to 3.5 ns. Given the similarity of this band to that identified at the same wavelength in the 0.1:1 film, the PA at 640 nm is again attributed to PC TTA. A direct comparison of the amplitude of the TTA in Figure 4A and Figure 2 (see also Figure IV-D, Supporting Information) clearly demonstrates, however, that the number of triplets formed in the 1:1 blend is significantly less than in the 0.1:1 blend. On the basis that the initial amplitude of the PA at 650 nm is the same in both films, it can be determined that (after 3.5 ns) there are [77 ± 3] % less triplets formed in the 1:1 blend as compared to the 0.1:1 blend. Furthermore, given that in section 3.1 Φ_T for the 0.1:1 blend was determined to be [95 ± 5] %, it follows that the corresponding yield in the 1:1 film is [31 ± 3] %.

To understand this origin of the reduced triplet yield, it is pertinent to consider the PB recovery of the 1:1 blend. The decay observed is identical to the corresponding recovery in the pristine PC material, as demonstrated in Figure 4B, with the exception that there is an additional long-lived component in the 1:1 film, which appears as a background offset in the kinetics. We attribute this to the fact that, following photoexcitation of the PC, there are a large number of excitons that recombine before reaching an active interface to undergo electron transfer, thus reducing the total number of polarons and triplet excitons formed. The properties of the singlet excitons are solely determined by the PC material alone and thus share identical recovery kinetics. It is clear this is the only mechanism by which the PC ground-state is recovered on such a time scale; the background offset can be attributed to the formation of triplet excitons, as discussed in the context of section3.1, and free polarons, as discussed above. From the magnitude of the background, it can be determined that [60 ± 5] % of the initial photoexcitation population are singlet excitons that decay before being able to undergo electron-transfer.

The PC singlet exciton PA extends from 700 nm to wavelengths shorter than 550 nm, as confirmed in measurements of the pristine film (see Figures I and II, Supporting Information) and will therefore overlap with both the PC^+ polaron PA and TTA bands in the 1:1 blend film. Note that the number of PC singlet excitons that live to 3.5 ns is very small and can be neglected in the analysis of the triplet yield as performed above. The overlap with the singlet exciton PA is, however, responsible for the absence of any isosbestic point at 600 nm, as was observed in the 0.1:1 blend. It is possible, however, to obtain an approximation of the pure kinetics of the polaron PA using the information above; namely, that 60% of the initial photoexcitation population are singlet excitons that recombine in PC domains. The details of this process are discussed in the Supporting Information. The extracted polaron PA kinetics at 540 nm in the 1:1 blend film is presented in Figure 4C, with the results of multiexponential fitting as applied to that data presented in Table 2. The corresponding results obtained at 550 nm in the 0.1:1 blend film are also included in Table 2 for ease of comparison.

In contrast to that observed at the same wavelength in the 0.1:1 blend, the kinetics at 540 nm in the 1:1 blend are characterized by a [6.3 ± 0.5] ps build-in component, which is indicative of the delayed formation of polarons. This can be attributed to the migration of excitons within the PC domains to interfacial regions, whereupon electron transfer and subsequently polaron formation occurs. Using the lifetime (τ) of the rise component and the lifetime data of the singlet PC excitons ([4.1 ± 0.5] ps; see Figure II, Supporting Information), the yield of excitons that decay before reaching an interface (Φ_{dec}) is calculated in the standard manner as

$$\Phi_{dec} = \frac{k_{S_1}}{k_{mig} + k_{S_1}} = \frac{\frac{1}{\tau_{S_1}}}{\frac{1}{\tau_{mig}} + \frac{1}{\tau_{S_1}}} = [61 \pm 9]\% \qquad (2)$$

This value of Φ_{dec} is the same as that obtained using the PB recovery at 750 nm and is further evidence for the validity of our analysis.

The remaining decay components of the PC^+ polarons in the 1:1 blend film are both longer than those obtained in the 0.1:1 blend and demonstrate an increase in the average electron−hole separation. There is no longer any evidence of order-10 ps recombination in the 1:1 film, indicating there are no GPP states that are tightly bound at an interface. Furthermore, the 120 component of the 0.1:1 blend film has increased to 177 ps in the 1:1 film. Finally, it can be seen that the increased separation of some states is such that the electron and hole can no longer be considered bound, giving rise to free polarons and the long decay component, which cannot be quantified by our experimental apparatus. Note that the background is [17 ± 5] % of the maximum polaron population, which is consistent with

dx.doi.org/10.1021/jp208820g | J. Phys. Chem. C 2012, 116, 4390−4398

the polaron yield of [12 ± 4] % measured at 950 nm. This is expected given that each band is due to the PA of PC^+ polarons, as established in section 3.1.

The increased electron−hole separation is consistent with the presence of percolation paths in the 1:1 blend, which did not previously exist in the 0.1:1 blend; these allow the PC^+ cation to move away from the interface at which it was generated. There are a number of studies within the literature that have explored similar issues. For example, in the work of Janssen et al. time-resolved photoluminescence spectroscopy was used to measure the lifetime of CT states in PF10TBT:PCBM blends for different PCBM doping concentrations.[18] As detailed therein, the lifetime of the CT emission was observed to decrease at higher doping ratios, accompanied by a simultaneous increase in the polaron yield. It was concluded that these increased electron−hole separations reported at higher doping ratios were due to increased electron mobility at high doping concentrations, which in turn were due to the formation of PCBM microcrystalline domains. The role of domain size in influencing the dissociation of GPP states has also been explored by Ruseckas et al. using time-resolved photoluminescence.[40] As a part of these studies, it was concluded that, in order for free polaron formation to occur, it was necessary for the average domain size to be larger than the coulomb capture radius of the GPP states; if the domain size was smaller than this limit, GPP recombination would prevail.

Taking these points together, we are now in a position to present a model of charge generation in the 1:1 blend film; this is outlined in Scheme 2. A large number of points remain, as in the 0.1:1 blend, and are not discussed further. The two key steps unique to the 1:1 film are as follows:

(1) Because of the increased PC domain size, the singlet exciton population generated following photoexcitation (1) must migrate to a PCBM interface before undergoing electron transfer. Because of the relatively short lifetime of the excitons, 60% of the initial singlet population are lost before this can occur.

(2) The increased PC domain size facilitates an increase in the average electron−hole separation following electron transfer. As a consequence, ∼15% of the GPP formed fully dissociate to become long-lived free polarons.

Scheme 2. Summary of Excited-State Kinetic Processes in the PC:PCBM (1:1 w/w) Film[a]

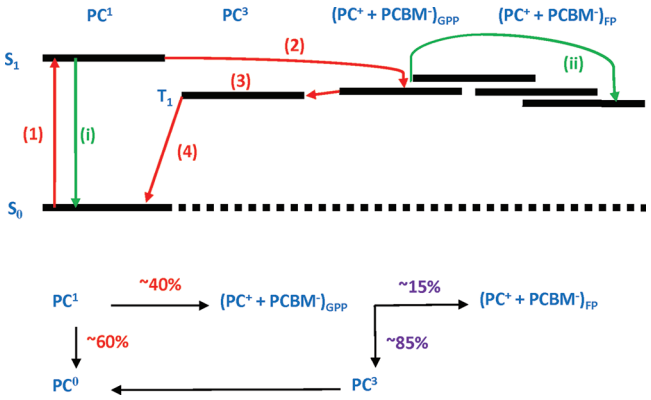

[a]Steps 1−4 are as described in Scheme 1. Green arrows are used to depict the processes that are unique to the 1:1 blend. Following photoexcitation of the PC moieties, 60% of excitons recombine (1) in larger (with respect to the 0.1:1 blend) domains before reaching an interface and undergoing electron transfer. In addition, due to an increase in the number of percolation paths in the 1:1 blend, ∼15% of the polaron pairs that are formed fully dissociate to become free polarons (FP, 2). A summary of the relevant branching ratios is included in the lower half of the scheme.

Using the branching ratios specified in points 1 and 2 above (see also Scheme 2), we determine that for the 1:1 film, Φ_T = [34 ± 9] %; the corresponding yield (with respect to the initial photoexcitation density) of free polarons (Φ_{FP}) is [6 ± 3] %. Note that the triplet yield is equal to that determined indirectly from the intensity of the TTA band ([31 ± 3] %), again demonstrating the consistency of our analysis.

It is clear that in the 1:1 film, GPP recombination to the triplet of the PC is still much more prominent that GPP dissociation into free polarons. As we are unable to distinguish between the PA of GPP and free polarons, we cannot comment on the relevant time scale of the dissociation process, which may give some clue as to why recombination accounts for 85% of all polaron states formed following electron transfer. The local morphology may play an important role in determining the branching ratio, as explored in the work of Inganäs et al.;[23] whereas in some regions, free polaron formation may occur due to high local charge mobility; in other regions, the charges may still be trapped in interfacial regions, giving rise to GPP recombination. In light of this, we are specifically only able to comment that there is an increase in the average electron−hole separation in the 1:1 blend.

At a more general level, it is clear that efficient GPP recombination to the triplet level of the PC in the 1:1 blend will fundamentally limit OPV device performance by reducing the number of free polarons that can be formed. This is the opposite situation to that in the extensively studied P3HT:PCBM system, in which the high OPV power conversion efficiency (∼5%)[1,2] can be partly ascribed to 100% efficient GPP dissociation.[21,27]

Efficient GPP recombination in the PC:PCBM system is expected to also have a significant impact on the operation of ternary blends, such as the popular P3HT:PC:PCBM system in which the PC is used to enhance solar capture in the infrared[7−9] and increase the harvest yield of singlet excitons generated in the polymer component via the so-called antenna effect.[10] In the work of Johansson et al., ultrafast transient absorption spectroscopy was performed in bulk-heterojunction P3HT:PC:PCBM blends in different blend ratios to establish a mechanism for charge generation.[11] They established that charge formation occurred in a two step process: (1) electron transfer from PC to PCBM, resulting in the formation of GPP states at the PC/PCBM interface, and (2) hole transfer from PC to P3HT, leading to the dissociation of said GPP states and the formation of free charges. The hole-transfer was established to occur on a range of time scales, spanning 1 ps to several hundred picoseconds. Having established in our work that the GPP recombination at the PC:PCBM interface occurs on a time scale as short as 20 ps, one would still expect to see recombination and triplet formation in the ternary blend, which would again act to reduce the free polaron yield. Indeed, we note that the prominent peak at 650 nm observed in the transient absorption spectra of that work may include some contribution from the TTA of the PC component, as opposed to the signature of P3HT polarons alone as concluded therein. We also expect that the effect of GPP recombination should

dx.doi.org/10.1021/jp208820g | J. Phys. Chem. C 2012, 116, 4390−4398

have an even more prominent role in bilayer architecture ternary systems, in which the enhanced phase segregation would give rise to longer hole-transfer times.

Our work also demonstrates that on a fundamental level, the relatively short lifetime of the PC singlet state results in a 60% loss of photoexcitations before electron transfer can occur, *even in a BHJ blend*. This is completely different to the properties of the 0.1:1 blend in which all excitons were quenched as a result of electron transfer within 400 fs, It is clear that there is a balance between favorable blend morphology for GPP dissociation and the loss of photoexcitations due to exciton decay. This process is particularly relevant in context of P3HT:PC:PCBM ternary blends and even more so for bilayer device architecture; while large PC contents may promote the NIR photon harvesting and the operation of the antenna effect, such systems will also simultaneously incur inherent population losses due to the decay of the PC singlet state.

4. CONCLUSIONS

In this article, we have employed femtosecond transient absorption spectroscopy to delineate the recombination and dissociation pathways of the GPP state formed following electron transfer in PC:PCBM BHJ blends. Significantly, GPP recombination occurs to the triplet state of the PC with high efficiency and is characterized by multiple time constants varying from ∼20 to 1000 ps. This range of lifetimes is indicative of a distribution of electron−hole distances in the GPP manifold, which is sensitive to the blend morphology. GPP dissociation into free polarons is also strongly dependent on the blend morphology and acts in competition with recombination to the triplet manifold. For the blends we measure herein, we report 0% free polaron generation in PC:PCBM 0.1:1 w/w blends and only 6% yield in 1:1 blends, whereas the yield of triplets in each case is found to be ∼100% and 32%. The low free polaron yield is a factor of both efficient GPP recombination and exciton recombination in PC domains, which occurs before electron transfer due to the relatively short lifetime of the PC singlet state. Both of these factors are expected to fundamentally reduce the OPV efficiency of both PC:PCBM and P3HT:PC:PCBM blends, particularly for bilayer architecture devices in which the phase segregation in enhanced.

■ ASSOCIATED CONTENT

Supporting Information

List of abbreviations; additional experimental details; comparison of the transient absorption spectra of pristine PC and transient absorption spectrum of P3HT:PC; results of independent fitting to selected data from Figure 2A; transient absorption spectrum of PC thin film and single-wavelength transient absorption kinetics of the singlet exciton photo-induced absorption band in the pristine PC film; determination of triplet yield in 0.1:1 blend film from photobleaching data; modification of kinetic data to account for spectral overlap. This material is available free of charge via the Internet at http://pubs.acs.org.

■ AUTHOR INFORMATION

Corresponding Author

*E-mail: e.w.snedden@durham.ac.uk.

Notes

The authors declare no competing financial interest.

■ ACKNOWLEDGMENTS

We thank Dr. Yonghao Zheng in the Department of Chemistry, Durham University, for electrochemical measurements. This work was supported by the EPSRC (grant number EP/I006656/1).

■ REFERENCES

(1) Kim, J. Y.; Lee, K.; Coates, N. E.; Moses, D.; Nguyen, T.-Q.; Dante, M.; Heeger, A. J. *Science* **2007**, *317*, 222−225.
(2) Kim, Y.; Cook, S.; Tuladhar, S. M.; Choulis, S. A.; Nelson, J.; Durrant, J. R.; Bradley, D. D. C.; Giles, M.; McCulloch, I.; Ha, C.-S.; Ree, M. *Nat. Mater.* **2006**, *5*, 197−203.
(3) Clarke, T.; Ballantyne, A.; Jamieson, F.; Brabec, C.; Nelson, J.; Durrant, J. *Chem. Commun.* **2009**, 89−91.
(4) Martinez-Diaz, M. V.; de la Torre, G.; Torres, T. *Chem. Commun.* **2010**, *46*, 7090−7108.
(5) Chu, C.-W.; Shrotriya, V.; Li, G.; Yang, Y. *Appl. Phys. Lett.* **2006**, *88*, 153504.
(6) Mutolo, K. L.; Mayo, E. I.; Rand, B. P.; Forrest, S. R.; Thompson, M. E. *J. Am. Chem. Soc.* **2006**, *128*, 8108−8109.
(7) Hardin, B. E.; Hoke, E. T.; Armstrong, P. B.; Yum, J.-H.; Comte, P.; Torres, T.; Frechet, J. M. J.; Nazeeruddin, M. K.; Gratzel, M.; McGehee, M. D. *Nat. Photonics* **2009**, *3*, 406−411.
(8) Dastoor, P. C.; McNeill, C. R.; Frohne, H.; Foster, C. J.; Dean, B.; Fell, C. J.; Belcher, W. J.; Campbell, W. M.; Officer, D. L.; Blake, I. M.; et al. *J. Phys. Chem. C* **2007**, *111*, 15415−15426.
(9) Peet, J.; Tamayo, A. B.; Dang, X. D.; Seo, J. H.; Nguyen, T. Q. *Appl. Phys. Lett.* **2008**, *93*, 163306−3.
(10) Honda, S.; Nogami, T.; Ohkita, H.; Benten, H.; Ito, S. *ACS Appl. Mater. Interfaces* **2009**, *1*, 804−810.
(11) Johansson, E. M. J.; Yartsev, A.; Rensmo, H.; Sundström, V. *J. Phys. Chem. C* **2009**, *113*, 3014−3020.
(12) Honda, S.; Yokoya, S.; Ohkita, H.; Benten, H.; Ito, S. *J. Phys. Chem. C* **2011**, *115*, 11306−11317.
(13) Loi, M. A.; Denk, P.; Hoppe, H.; Neugebauer, H.; Winder, C.; Meissner, D.; Brabec, C.; Sariciftci, N. S.; Gouloumis, A.; Vazquez, P.; Torres, T. *J. Mater. Chem.* **2003**, *13*, 700−704.
(14) Coffey, D. C.; Ferguson, A. J.; Kopidakis, N.; Rumbles, G. *ACS Nano* **2010**, *4*, 5437−5445.
(15) Thompson, B. C.; Frechet, J. M. J. *Angew. Chem., Int. Ed.* **2008**, *47*, 58−77.
(16) Deibel, C.; Strobel, T.; Dyakonov, V. *Adv. Mater.* **2010**, *22*, 4097−111.
(17) Clarke, T. M.; Durrant, J. R. *Chem. Rev.* **2010**, *110*, 6736−6767.
(18) Veldman, D.; Ïpek, O. Z.; Meskers, S. C. J.; Sweelssen, J. R.; Koetse, M. M.; Veenstra, S. C.; Kroon, J. M.; Bavel, S. S. V.; Loos, J.; Janssen, R. A. J. *J. Am. Chem. Soc.* **2008**, *130*, 7721−7735.
(19) Hallermann, M.; Da Como, E.; Feldmann, J.; Izquierdo, M.; Filippone, S.; Martin, N.; Juchter, S.; von Hauff, E. *Appl. Phys. Lett.* **2010**, *97*, 023301−3.
(20) Tvingstedt, K.; Vandewal, K.; Gadisa, A.; Zhang, F.; Manca, J.; Inganäs, O. *J. Am. Chem. Soc.* **2009**, *131*, 11819−11824.
(21) Hallermann, M.; Kriegel, I.; Como, E. D.; Berger, J. M.; Hauff, E. V.; Feldmann, J. *Adv. Funct. Mater.* **2009**, *19*, 3662−3668.
(22) Tvingstedt, K.; Vandewal, K.; Gadisa, A.; Zhang, F.; Manca, J.; Inganäs, O. *J. Am. Chem. Soc.* **2009**, *131*, 11819−11824.
(23) Tvingstedt, K.; Vandewal, K.; Zhang, F.; Inganäs, O. *J. Phys. Chem. C* **2010**, *114*, 21824−21832.
(24) Vandewal, K.; Tvingstedt, K.; Gadisa, A.; Inganäs, O.; Manca, J. V. *Nat. Mater.* **2009**, *8*, 904−909.
(25) Ohkita, H.; Cook, S.; Astuti, Y.; Duffy, W.; Heeney, M.; Tierney, S.; McCulloch, I.; Bradley, D. D. C.; Durrant, J. R. *Chem. Commun.* **2006**, 3939−3941.
(26) Brabec, C. J.; Zerza, G.; Cerullo, G.; De Silvestri, S.; Luzzati, S.; Hummelen, J. C.; Sariciftci, S. *Chem. Phys. Lett.* **2001**, *340*, 232−236.
(27) Guo, J.; Ohkita, H.; Benten, H.; Ito, S. *J. Am. Chem. Soc.* **2010**, *132*, 6154−6164.

(28) Kaneko, Y.; Arai, T.; Sakuragi, H.; Tokumaru, K.; Pac, C. *J. Photochem. Photobiol., A* **1996**, *97*, 155−162.
(29) Rothe, C.; Monkman, A. *J. Chem. Phys.* **2005**, *123*, 244904.
(30) Kondakov, D. Y. *J. Appl. Phys.* **2007**, *102*, 114504.
(31) Rothe, C.; Al Attar, H. A.; Monkman, A. P. *Phys. Rev. B* **2005**, *72*, 155330.
(32) Guo, J. M.; Ohkita, H.; Yokoya, S.; Benten, H.; Ito, S. *J. Am. Chem. Soc.* **2010**, *132*, 9631−9637.
(33) Keivanidis, P. E.; Kamm, V.; Dyer-Smith, C.; Zhang, W.; Laquai, F.; McCulloch, I.; Bradley, D. D. C.; Nelson, J. *Adv. Mater.* **2010**, *22*, 5183−5187.
(34) Frackowiak, D.; Planner, A.; Waszkowiak, A.; Boguta, A.; Ion, R.-M.; Wiktorowicz, K. *J. Photochem. Photobiol., A* **2001**, *141*, 101−108.
(35) King, S. M.; Rothe, C.; Dai, D.; Monkman, A. P. *J. Chem. Phys.* **2006**, *124*, 234903.
(36) Baigel, D. M.; Gorman, A. A.; Hamblett, I.; Hill, T. J. *J. Photochem. Photobiol., B* **1998**, *43*, 229−231.
(37) Gélinas, S.; Paré-Labrosse, O.; Brosseau, C.-N.; Albert-Seifried, S.; McNeill, C. R.; Kirov, K. R.; Howard, I. A.; Leonelli, R.; Friend, R. H.; Silva, C. *J. Phys. Chem. C* **2011**, *115*, 7114−7119.
(38) Pal, S. K.; Kesti, T.; Maiti, M.; Zhang, F.; Inganäs, O.; Hellström, S.; Andersson, M. R.; Oswald, F.; Langa, F.; Österman, T.; et al. *J. Am. Chem. Soc.* **2010**, *132*, 12440−12451.
(39) Bredas, J.-L.; Norton, J. E.; Cornil, J.; Coropceanu, V. *Acc. Chem. Res.* **2009**, *42*, 1691−1699.
(40) Ruseckas, A.; Shaw, P. E.; Samuel, I. D. W. *Dalton Trans.* **2009**, 10040−10043.